

Hadron Component in Air showers at Mt. Chacaltaya Experiment

C. Aguirre¹, K. Hashimoto², K. Honda³, N. Inoue⁴, N. Kawasumi², Y. Maeda⁵,
N. Martinic¹, T. Matano⁶, N. Ohmori⁵, A. Ohsawa⁷, K. Shinozaki⁴, M. Tamada⁸,
R. Ticona¹, I. Tsushima² and K. Yokoi⁹

¹*Institute de Investigaciones Fisicas, Universidad Mayor de San Andres, La Paz, Bolivia*

²*Faculty of Education, Yamanashi University, Kofu, 400-8510 Japan*

³*Faculty of Engineering, Yamanashi University, Kofu, 400-8511 Japan*

⁴*Faculty of Science, Saitama University, Urawa, 338-8570 Japan*

⁵*Faculty of Science, Kochi University, 780-8520 Japan*

⁶*Tanashi, Tokyo, 188-0014 Japan*

⁷*Institute for Cosmic Ray Research, University of Tokyo, Tanashi, 188-8502 Japan*

⁸*Faculty of Science and Technology, Kinki University, Higashi-Osaka, 577-8502 Japan*

⁹*Faculty of Science and Technology, Aoyama University, Setagaya, Tokyo, 157-8572 Japan*

1 Introduction:

The experiment to operate an air shower array, a hadron calorimeter and an emulsion chamber is carried out at Mt. Chacaltaya (5200 m, Bolivia). The emulsion chamber detects high energy particles in the air shower, called 'family'. In this way the experiment supplies us with the data of the air shower together with those of high energy particles in the air shower simultaneously.[1]

In our previous article we have reported the details of the experimental procedure and discussed mainly the relation between the families and the accompanied air showers.[1]

In the present article we discuss the data from hadron calorimeter which is located beneath the emulsion chamber of 15 cm Pb thick. The plastic scintillator of the hadron calorimeter detects the charged particles which traverse the detector. Because an electron (or a photon), incident upon the emulsion chamber, can hardly produce electrons which arrive at the hadron calorimeter, these charged particles are produced by the hadron component, incident upon the chamber, through nuclear cascade process in the chamber. In this way the hadron calorimeter supplies the data of hadron component in the air shower.

The hadron calorimeter consists of 32 units of plastic scintillator (50 cm × 50 cm × 5 cm each), which are located beneath the emulsion chamber. The roles of the hadron calorimeter are to detect charged particles, produced by hadron component in the air shower, and to supply us with a clue to relate the families, which have no data of the arriving time, with the air showers. That is, the family is related to the hadron component through their center position, and the hadron component is related to the air shower through their arriving time.

2 Experimental data:

Each unit of the hadron calorimeter measures the energy deposit in the scintillator, which is converted to (charged) particle number using the average energy loss of a single muon in the scintillator. Thus each unit measures the charged particle density n_b , *i.e.*, the number of charged particles per area of 50 cm × 50 cm, called 'particle density' hereafter. Consequently the hadron calorimeter of 32 units measures the lateral distribution of the particle density. Each unit of the detector is sensitive to the particle density of $10 \sim 10^5$ particles.

The data by the air shower array and by the hadron calorimeter are recorded when at least one unit of the hadron calorimeter has the particle density exceeding 10^3 particles.

Among the recorded events those in which at least one of hadron calorimeter has the particle density exceeding 10^4 particles are selected for the present analysis. The number of selected events is 2408 for 4.6 years (May 1979 - Nov. 1985), during which the emulsion chamber is operated simultaneously. The present set of data is not biased in the air shower size region of $N_e > 5 \times 10^6$.

3 Lateral distribution of particle density:

3.1 The lateral distribution of the particle density: The lateral distribution of the particle density is determined from the particle density data of respective events. Principally it is to look for the least square fitting to the curve,

$$n(r) = \frac{A}{r_0^2} \left(\frac{r}{r_0} \right)^{-\alpha} \quad (r_0 = 1 \text{ (m)}) \quad (1)$$

Thus the parameter A and α of Eq.(1), together with the center of the distribution, are determined for each event. The distance between the center of the particle density, thus determined, and the air shower center is 0.9 ± 0.7 (m), which shows that both agree well taking into account the error of the air shower core determination.

Fig. 1 shows the lateral distributions of the average particle density in the size regions of $N_e = 5 \times 10^6 \sim 10^7$ and $10^7 \sim 5 \times 10^7$. The average particle density is obtained by calculating the particle densities at $r = 0.2, 0.3, 0.5, 0.7, 1.2, 2.0, 3.0$ and 5.0 (m), from the parameters A and α for each event. (The raw data of the particle density lie in the region $r = 0.5 \sim 5$ (m).)

3.2 Lateral distribution of the particle density by the hadrons in the air shower:

Being modeled upon the electromagnetic cascade theory, we assume that the number of hadrons with the energy between E and $E + dE$ in the area $r d\phi dr$ at the distance r from the center is given approximately by

$$F(E, r)dE = \frac{N_0}{\pi} \left(\frac{E}{E_c} \right)^{-\gamma-1} \frac{dE}{E} \frac{1}{\left(\frac{K}{E} \right)^2 - \left(\frac{K}{E_2} \right)^2} \theta(K - Er) \quad (2)$$

where $\theta(x)$ is the step function.

The constant K , which specifies the lateral spread of hadrons in the air shower as $K = (2/3) \langle Er \rangle$, depends approximately on the average value of the transverse momentum of the produced particles in multiple particle production $\langle p_T \rangle = 0.4$ (GeV/c) and 1 collision mean free path of the air at Mt. Chacaltaya $\lambda_{coll} = 1.6$ (km) as $K = \langle p_T \rangle \lambda_{coll} = 0.64$ (TeV m).

When a single pion of the energy E_0 enters the emulsion chamber of 15 cm Pb thick, the particle number, detected by the hadron calorimeter, is given by[2]

$$N_{hc}(E_0) = \left(\frac{E_0}{E_c} \right)^\beta \quad (\beta = 1.0, \quad E_c = 0.56 \text{ GeV}) \quad (3)$$

Consequently, when the pions, incident upon the chamber, are distributed as $F(E, r)dE$ of Eq.(2), the particle density distribution, detected by the hadron calorimeter, is

$$n(r) = \frac{N_0}{\pi(\beta - \gamma + 2)} \left(\frac{E_c}{K} \right)^2 \left(\frac{K}{E_c r} \right)^{\beta - \gamma + 2} \quad (4)$$

which is consistent with the empirical distribution of $r^{-\alpha}$ in Eq.(1).

3.3 Differential number of hadrons: Because the particle density is observed in the distance of $r = 0.5 \sim 5.0$ (m), the corresponding energy region is $E = 0.1 \sim 1$ (TeV). Hence we use the differential number of hadrons at $E = 1$ TeV for the purpose of the various comparisons, made below. It is given by

$$n_h \equiv \left(\frac{dN_h}{dE} \right)_{1 \text{ TeV}} = \pi \alpha A \left(\frac{K}{1 \text{ TeV}} \right)^{2-\alpha} \left(\frac{E_c}{1 \text{ TeV}} \right)^\beta \frac{1}{1 \text{ TeV}} \quad (5)$$

Fig. 2 shows the differential energy spectrum of hadrons in the air showers of $N_e = 5 \times 10^6 \sim 10^7$, together with the simulation. The simulation assumes the 'normal' composition for the primary cosmic rays and UA5 algorithm for nuclear interactions in the atmosphere.[3] It predicts a larger number of hadrons than the experimental data, which is found for the high energy γ -rays in the air shower, too.[1]

4 Primary cosmic-ray composition in 10^{16} eV:

Fig. 3(a) shows the distribution of n_h (the differential number of hadron at $E = 1$ TeV) for 62 air showers which have the size of $N_e = 5 \times 10^6 \sim 10^7$ and age parameter of $s = 0.6 \sim 0.8$. The former criterion assures that the sampled air showers are not biased by the hadron calorimeter triggering mode, and the latter does that the air shower size is proportional to the energy of the primary particle approximately irrespective of the characteristics of the primary particle.

Fig. 3(b) shows the distribution of n_h (on the log-scale) for 202 events by the simulation.[3] The log-scale of n_h is convenient for us to discuss the distribution of n_h , leaving the absolute value of n_h , because the absolute value of n_h does not agree with that of the simulation.

Fig. 3(c) shows n_h distributions of the proton-induced and iron-induced events by the simulation. One can see that the left-hand side of the distribution consist only of the proton-induced showers, which enables us to estimate the fraction of proton-induced events. And both distributions of proton-induced and iron-induced events is approximated well by the normal distribution with the dispersions of $\sigma_{proton} = 0.183$ and $\sigma_{iron} = 0.107$.

Fig. 3(d) shows n_h distributions of the experiment and proton-induced events by the simulation in integral form. One can estimate the number of proton-induced events is 45 ± 5 , which correspond to 73 ± 8 % among the total observed events.

References

- [1] N. Kawasumi et al., Phys. Rev. D53 (1996) 3534.
- [2] C. Aguirre et al., Nucl. Phys. B (Proc. Suppl.) (Gran Sasso) to be published.
- [3] M.Tamada, J. Phys. G20 (1994) 487.

Figure captions

Fig. 1 Lateral distribution of average particle density for the air showers of $N_e = 10^{6.7 \sim 7}$ (below) and $N_e = 10^{7 \sim 7.7}$ (above).

Fig. 2 Energy spectrum of hadrons, obtained from the lateral distribution of the particle density. (The solid line is the experimental data.)

Fig. 3(a) n_h distribution of the experimental data.

Fig. 3(b) n_h distribution by the simulation.

Fig. 3(c) n_h distributions of proton-induced and iron-induced events among the simulated events.

Fig. 3(d) n_h distribution in integral form. (The lines are for proton-induced events where the figures, attached to the curves, are the number of events.)

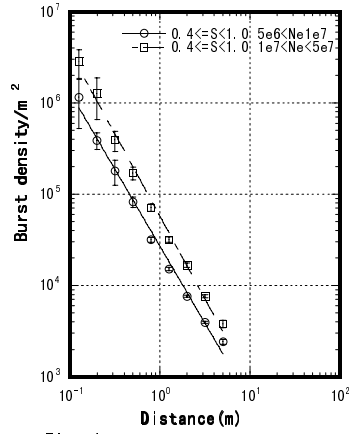


Fig. 1

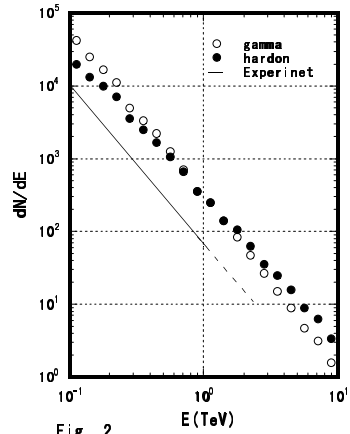


Fig. 2

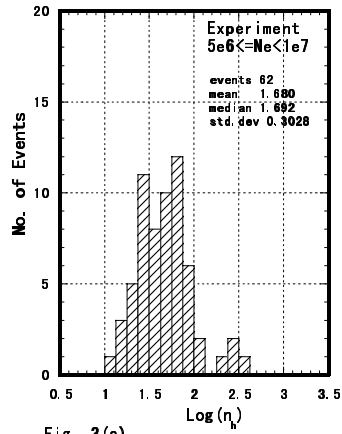


Fig. 3(a)

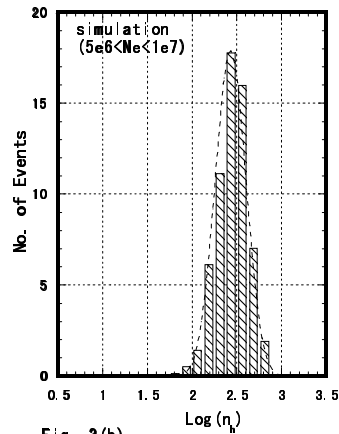


Fig. 3(b)

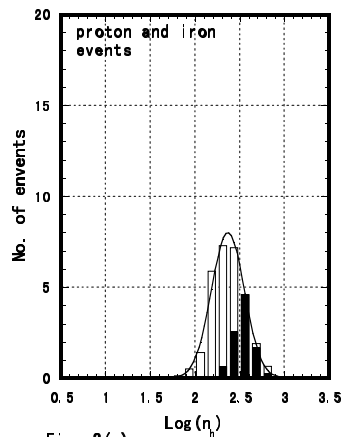


Fig. 3(c)

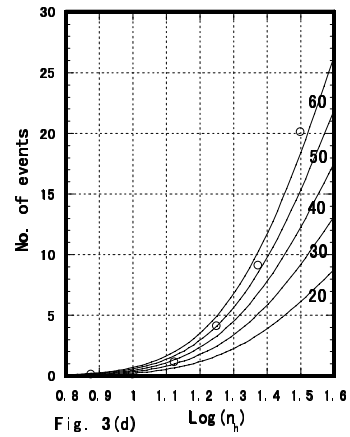


Fig. 3(d)